Regular Article

ORGANIC CHEMISTRY RESEARCH
Published by the
Iranian Chemical Society
www.orgchemres.org

Org. Chem. Res., Vol. 5, No. 1, 32-41, March 2019.

An Experimental Study to Biological Activity and Synthesis; and Theoretical Study for MEP, HOMO/LUMO Analysis and Molecular Docking of *N*-(2-pyridyl)-*para*-styrene Sulfonamides

P. Shafieyoon[a], E. Mehdipour[a,*] and H. Tavakol[b]

[a]*Department of Chemistry, Faculty of Science, Lorestan University, Khoramabad, Iran*

[b]*Department of Chemistry, Isfahan University of Technology, Isfahan 84156-83111, Iran*

(Received 4 February 2018, Accepted 11 August 2018)

A combined experimental and theoretical investigation has been performed on *N*-(2-pyridyl)-*para*-styrene sulfonamide (abbreviated as PSS). This compound was synthesized from the reaction of *para*-styrene sulfonyl chloride and 2-amino pyridine. The PSS was confirmed using FT-IR, and ^{1}H NMR spectroscopies. MEP and HOMO-LUMO analyses of the PSS have been performed using DFT method. The PSS is investigated against Staphylococcus aureus and Escherichia coli. Molecular docking study is also reported.

Keywords: *N*-(pyridyl)-*para* styrene sulfonamide, DNA, BSA, MEP, HOMO and LUMO analysis

INTRODUCTION

Sulfonamides are important and significant groups of drugs. They possess interesting biological activities [1,2] including antimicrobial [3-5] and anticancer activities [6-8]. In addition, some particular activities have been observed for their derivatives such as anticancer properties in thiadiazolo [9], pyrimidines [10] and *N*-alkyl-*N*- [(8-R-2,2-dimethyl-2*H*-chromen-6-yl) methyl] heteroarylsulfonamides [11], and also anti-inflammatory properties in *para*-substituted *N*-benzenesulfonyl derivatives of anthranilic acid [12]. In this respect, some sulfonamide derivatives have been employed as pharmacological agents in antibacterial [13-18] diabetes treatment [19-24] and antithyroid drugs [25,26]. Therefore, the clinical and medicinal importance of sulfonamides are well known. It has been accepted that by changing the structural parts of the sulfonamide, new drugs have been designed in the recent investigations [27]. They have been used for different purposes such as antitumor [28,29] and antiviral [30,31] activities. Acyl sulfonamide derivatives have been also reported as influenza neuraminidase inhibitors [32].

*Corresponding author. E-mail: mehdipour.e@lu.ac.ir

These results promoted us to synthesize and evaluate a new series of sulfonamide derivatives for medicinal and pharmaceutical chemistry. Our previous reports were related to the spectral and theoretical investigation about the new drug-based materials [33,34]. To this end, we have selected pyridine and styrene structural parts to synthesize our especial sulfonamide structure due to coordination to metals and preparation of new complex-based sulfonamide drugs [35,36] This complex has the medicinal as well as the catalytic properties. It can be attached to the target macromolecule (DNA and BSA), as a simple drug will be used [37]. In addition, in organometallic chemistry, metal complexes containing sulfonamides ligands are interesting complexes that have been used as efficient catalysts in organic syntheses. Our previous report was related to palladium complex, its crystal structure and mixed ligand [38-41]. The electron withdrawing character of the sulfonyl group increases the acidic character of the NH group and makes the process of ligand deprotonation easier. Therefore, these ligands can be coordinated to the metal atom in several ways. In this research, we report a synthesis, some of the theoretical and experimental investigations, and molecular docking ability (DNA and BSA) of *N*-(2-pyridyl)-4-styrene sulfonamide.

MATERIAL AND METHODS

Para-vinyl benzene sulfonic acid sodium salt, PCl_5, sodium hydroxide, $CHCl_3$ and 2-amino pyridine were purchased from Merck and Sigma-Aldrich companies and were used without further purification. Fourier transform infrared spectra of the prepared compounds were recorded at 400-4000 cm^{-1} region using KBr pellets on Shimadzu FT-IR 8400 spectrometer. ^1H NMR spectrum was recorded on a Brucker Ultrashield 400 MHz spectrometer using DMSO-d_6 as solvent and tetramethylsilane as internal standard.

Preparation of *Para*-styrene Sulfonyl Chloride

The desired compound was prepared as the previously described method with some minor changes [42]. For this purpose, 5 g (24 mmol) of *para*-vinyl benzene sulfonic acid sodium salt and 7.5 g (36 mmol) of PCl_5 were placed in a 50 ml round-bottomed flask equipped with a magnetic stirrer. After 10 minutes, the mixture converts to oily liquid. The reaction mixture was stirred for 3 h at 50 °C temperature. Then, the residue was poured into ice-water, mixed and neutralized with excess of 10% NaOH solution and extracted using chloroform. The product was washed 3 times with water. The solvent was evaporated and product used without further purification.

Preparation of N-(2-pyridyl)-4-styrene Sulfonamide (PSS)

The synthetic method for the preparation of the title compound (PSS with chemical formula $C_{13}H_{12}N_2O_2S$) is as follows: 4.86 g *para*-styrene sulfonyl chloride (24 mmol), 2.25 g 2-amino pyridine (24 mmol), NaOH 1 M (24 ml) and $CHCl_3$ (50 ml, used as solvent) were placed in a 100 ml round-bottomed flask, equipped with magnetic stirrer. The reaction mixture was stirred for 4 h at room temperature. After this time, the solvent was evaporated and PSS as the product was obtained. The obtained product was washed 3 times with methanol and analyzed without further purification. (yield 4.74 g, 76.0%, m. p.: 207 °C). IR (KBr, cm^{-1}): 3340(m), 3057(m), 3028(m), 1631(s), 1600(m), 1529(m), 1460(m), 1388(s), 1356(s), 1276(m), 1138(s), 1084(m), 999(m).

^1H NMR (DMSO-d_6, ppm): 3.40 (NH), 5.45 (CH in vinyl), 6.01 (CH in vinyl), 6.82 (CH in vinyl), 7.67 (CH Benzene) 7. 88 (CH Benzene), 6.91, 7.21, 7.77 and 8.04 (pyridine ring).

Computational Details

Calculations of the PSS were performed using Gaussian 09 software [43]. These calculations include geometry optimization (opt-freq), MEP, HOMO-LUMO analyses were performed using density functional theory (DFT) [44, 45]. The optimizations (opt-freq) of all structures (tautomers) were carried out at the CAM-B3LYP/Aug.-cc-pVDZ level of theory. PASS (prediction of activity spectra) [46] was used as an online server to predict the activity of the ligand. Molecular docking has recently been used as a tool to gain further insight into the ligand-receptor interactions and screen molecules for the binding affinities against a special receptor. Molecular docking calculations were performed using AutoDock-Vina software [47]. The output of geometry optimization (using CAM-B3LYP/Aug-cc-pVDZ level of theory) for title compound was used as the input of ligand for docking processes. Lamarckian Genetic Algorithm (LGA) available in Autodock was employed for docking, as the most popular algorithm [48, 49]. The 3D crystal structure of employed DNA and BSA as receptors were obtained from Protein Data Bank (PDB ID: 423D, 4F5S). The graphical representation of ligand-receptor interaction was obtained using LigPlot software [50].

Antibacterial Assays

The minimal inhibitory concentration (MIC) of the PSS as an antibacterial agent against Escherichia coli and Staphylococcus aureus is discussed in the following section. The ASS was tested for its antibacterial activity against Staphylococcus aureus, as the model from Gram-positive and Escherichia coli as Gram-negative bacteria by the disk diffusion method [51].

Preparation of Nutrient-Agar Medium

3.80 g of Nutrient-Agar (NA) medium was dissolved in 100 ml of distilled water. This solution was sterilized at 120 °C for 20 min in an autoclave. Then, 20 ml of this solution was solidified in Petri plate.

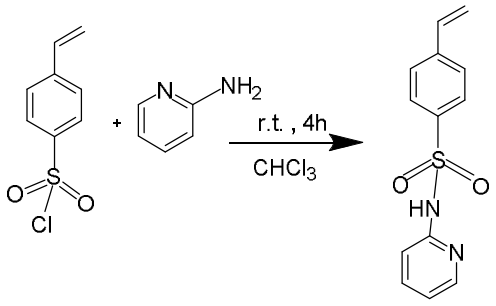

Scheme 1. The reaction involving synthesis of PSS

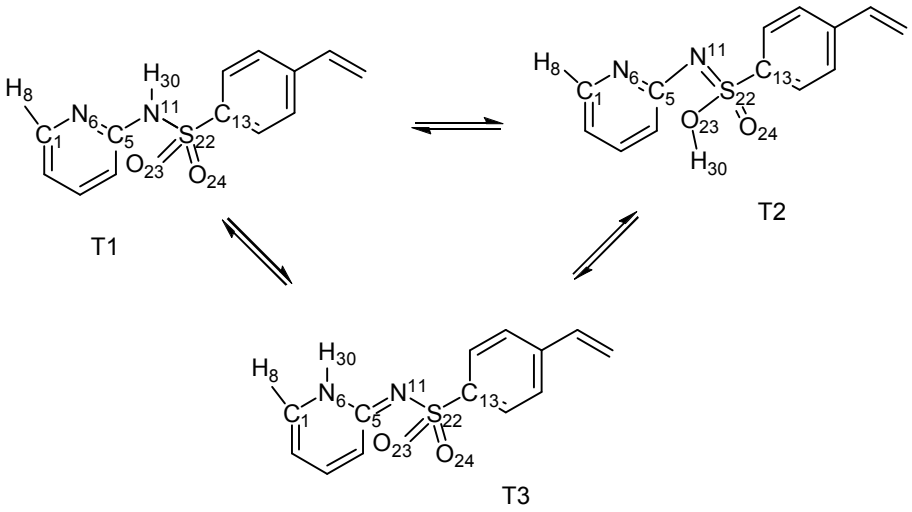

Fig. 1. The general structures of PSS tautomers.

Table 1. Kinetic and Thermodynamic Data of Three Tautomers

Tautomer	HF energy	ZPE	Relative total E	Relative H	Relative G
T_1	0	0	0	0	0
T_2	24.18	-1.1	23.12	23.4	23.34
T_3	1.84	0.13	1.97	1.89	1.89

All energetic data have been reported in kcal mol^{-1}.

RESULTS AND DISCUSSION

Synthesis and Characterization

PSS was prepared by reactions of *para* styrene sulfonyl chloride with 2-amino pyridine in the presence of $CHCl_3$ as solvent and NaOH in the room temperature (Scheme 1). The new ligand was characterized by FT-IR and ^1H NMR spectroscopy (data in the experimental section).

Tautomeric and Dynamic Processes

PSS could be presented in three different tautomers (named as T_1, T_2, T_3). The relative stabilities of these tautomers are of particular importance.

In this respect, structures of these tautomers were calculated at the CAM-B3LYP/Aug.-cc-pVDZ level of theory. Thermodynamic properties such as HF energies, relative enthalpies, relative total energies and relative Gibbs free energies for three tautomers (T_1, T_2 and T_3) are shown in Table 1. As a result, T_1 tautomer is the most stable structure, due to the aromaticity in pyridine ring and the symmetrical elements in SO_2.

Spectroscopic Characterization of PSS

The experimental FT-IR of PSS was presented in section 2.2 (Fig. 2). The C-H stretching frequencies of aromatic can be observed in the range of 3000-3100 cm^{-1} as shown at 3057 cm^{-1}. The C=N and C= C stretching vibrations are in the range of 1430-1650 cm^{-1}. In addition, the stretching mode of NH group is appeared at 3340 cm^{-1}. In the following discussion, sulfonamides are absorbed strongly at 1155-1170 and 1335-1370 cm^{-1}. The symmetrical and asymmetrical stretching mode of O=S=O are observed at 1138$cm^{-1}$and 1388 cm^{-1}, respectively.

Observed NMR Chemical Shifts

The experimental ^1H NMR spectrum of the title compound was provided in section 2.2. The ^1H NMR spectrum of the PSS was recorded in DMSO-d6 as solvent with TMS as internal standard at 400 MHz (Fig. 3). [2.50 related to DMSO-d6 as solvent (supply 1)].

Molecular Electrostatic Potential

Molecular electrostatic potential (MPE) is as an important tool to predict the electrophilic and nucleophile attacks in the biological interactions. The MEP of the title compound optimized geometry using CAM-B3LYP method and Aug -cc-pVDZ basis set. As can be seen in Fig. 4, the different colors in this plot indicate different values of the electrostatic potential; red < orange < yellow < green < blue. The blue color demonstrates the strongest attraction. The positive area is located around vinyl and phenyl groups. These areas have positive potential. The negative area belongs to pyridyl group and SO_2. These areas, having negative potential, are over the electronegative atoms such as oxygen and nitrogen atoms. The red color indicates the strongest repulsion. These regions of negative potential are associated with the lone pair of electronegative atoms. The residual species are surrounded by zero potential.

Frontier Molecular Orbital Analysis

Investigation of the HOMO and LUMO is important in a molecule as a ligand. The LUMO energy explains the ability of electron acceptation and the HOMO energy is related to the ability of electron donation. The HOMO and LUMO play a significant role in the electrical properties and chemical activities in the compound. The HOMO and LUMO orbital energies are important parameters to predict the chemical properties of the title compound. The HOMO and LUMO orbital energies of PSS are calculated at the B3LYP method and 6-311+g (p, d) basis set. Energy values are E_{HOMO} = -8.203 and E_{LUMO} = -0.957 eV. Energy difference between the HOMO and LUMO is 7.246 eV. The energies of HOMO and LUMO orbitals of the PSS are negative indicating that this compound is stable and does not decompose spontaneously into its elements. The energy gap is HOMO-LUMO = 7.246 eV. According to Parr *et al.* [52], the larger the HOMO-LUMO energy gap, the harder the molecule. A molecule with a high energy gap is less polarizable, has high kinetic stability and is termed as a hard molecule. The hardness (weakly polarizable) can be explained as the resistance towards the deformation of electron cloud and polarization of chemical systems during the chemical process. The chemical hardness is a useful concept for predicting the behavior of chemical systems and is related to the stability and reactivity of a chemical system. Using HOMO and LUMO orbital energies, the ionization energy and electron affinity can be calculated as: $I = -E_{HOMO} = 8.203$ and $A = -E_{LUMO} = 0.957$ eV. The global hardness η and chemical potential μ are given using the equations $\eta = (I - A)/2 = 3.623$ eV and $\mu = -(I + A)/2 = -4.58$ eV, and the electrophilicity index by equation $(\omega) = \mu^2/2\eta = 2.894$ eV. The calculated value describes the biological activity of the title compound. Atomic orbital components of the frontier molecular orbital are shown in Fig. 5.

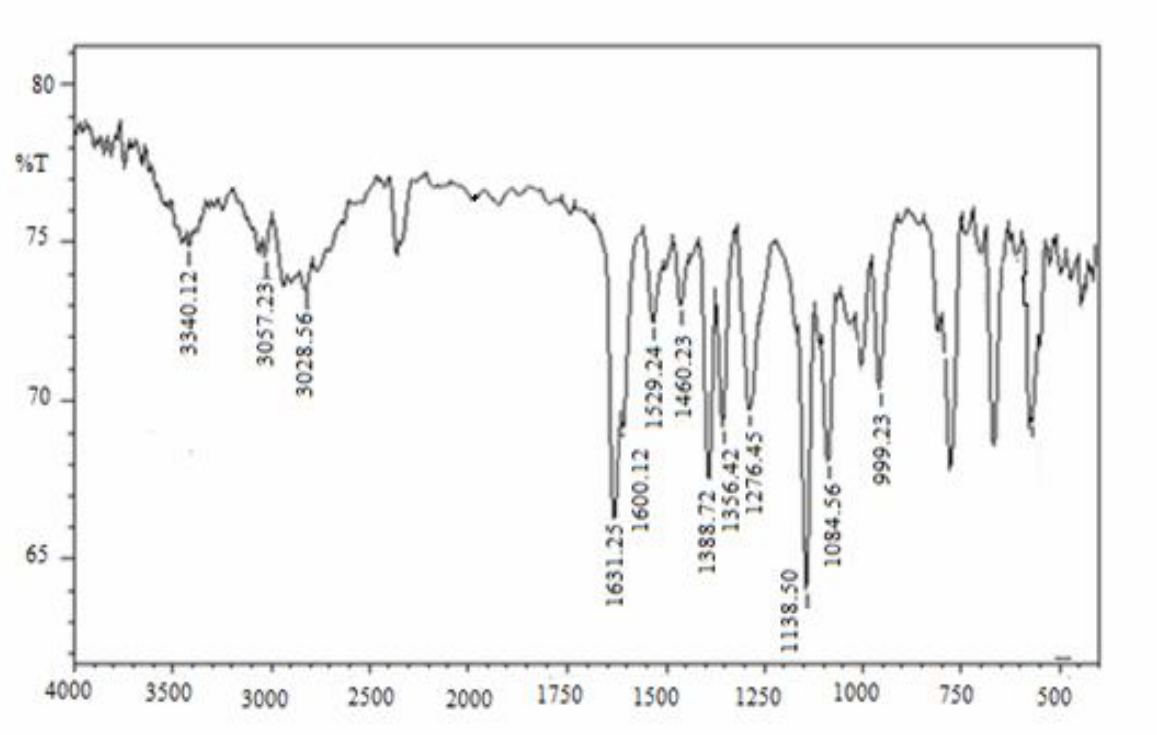

Fig. 2. The experimental FT-IR of PSS.

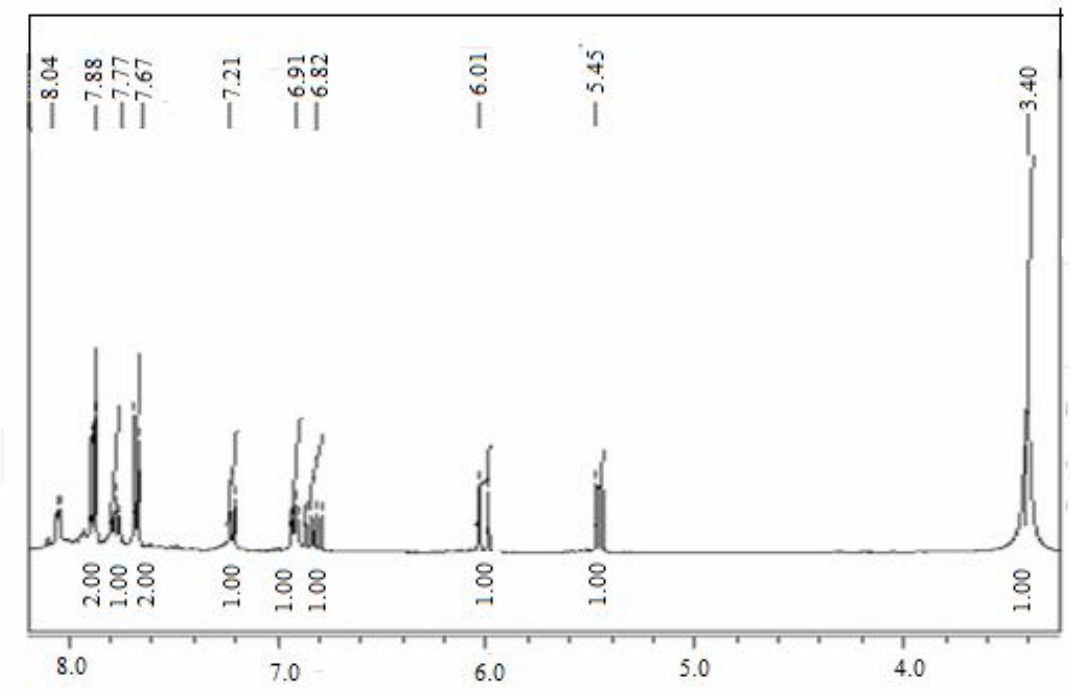

Fig. 3. The experimental ^{1}H NMR of PSS.

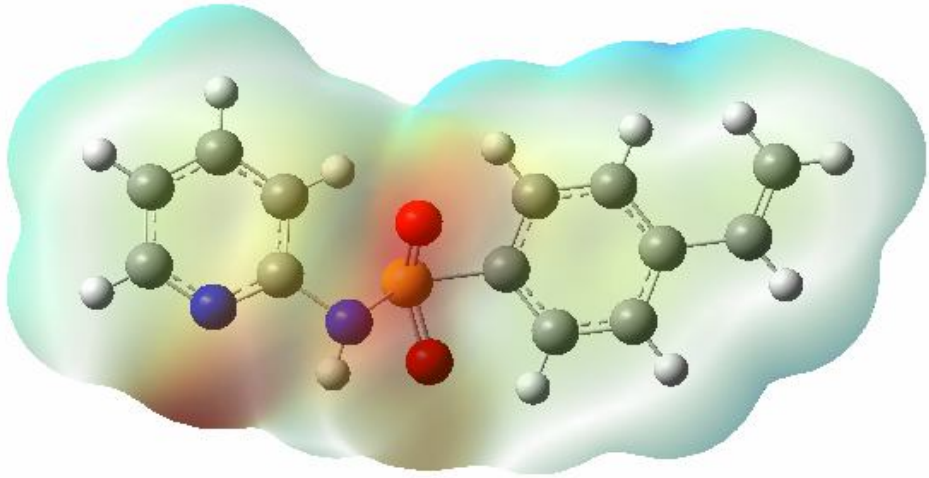

Fig. 4. MEP plot of *N*-(pyridyl) *para* styrene sulfonamide.

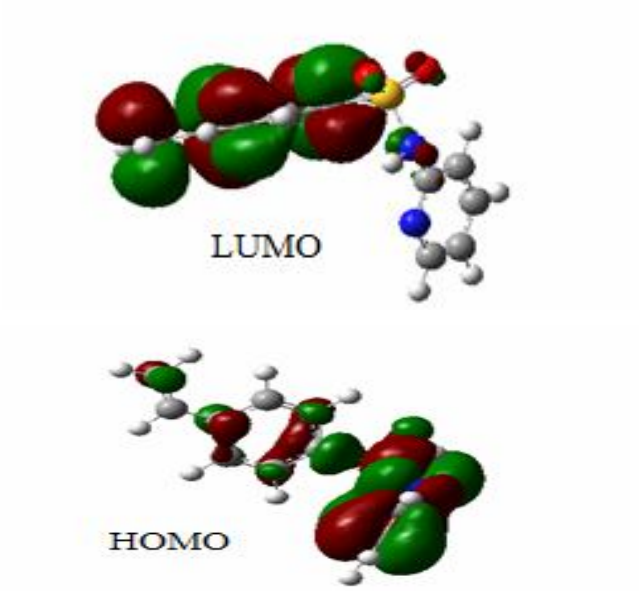

Fig. 5. HOMO and LUMO plots of *N*-(pyridyl)-p-styrene sulfonamide.

Molecular Docking Studies

We performed molecular docking simulation of the title compound against the 3D crystal structure of DNA and BSA obtained from Protein Data Bank (PDB ID: 423D, 4F5S), respectively. Molecular docking is a significant investigation to understand the ligand- receptor interactions. The ligand was prepared for docking using CAM-B3LYP method and Aug-cc-pVDZ basis set. The active sites of the DNA and BSA were defined to include residues of the active site within the grid box size of 30 Å × 28 Å × 42 Å for DNA and 88 Å × 64 Å × 74 Å for BSA with a grid-point spacing of 1.00 Å. Among the docked conformations, the best scored conformation, predicted by AutoDock scoring function, was visualized for ligand-DNA and ligand-BSA interactions in Ligplot and Ligplus softwares. The docking study on the PSS-DNA system showed that the PSS places in the major groove of DNA. The resulting docking in which the ligand binds into the DNA creates one hydrogen

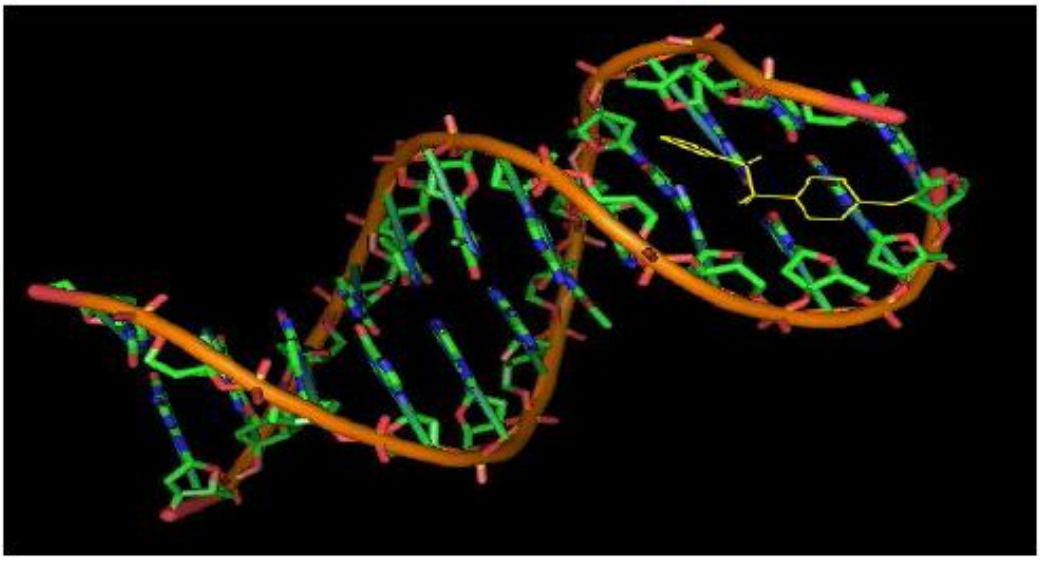

(A)

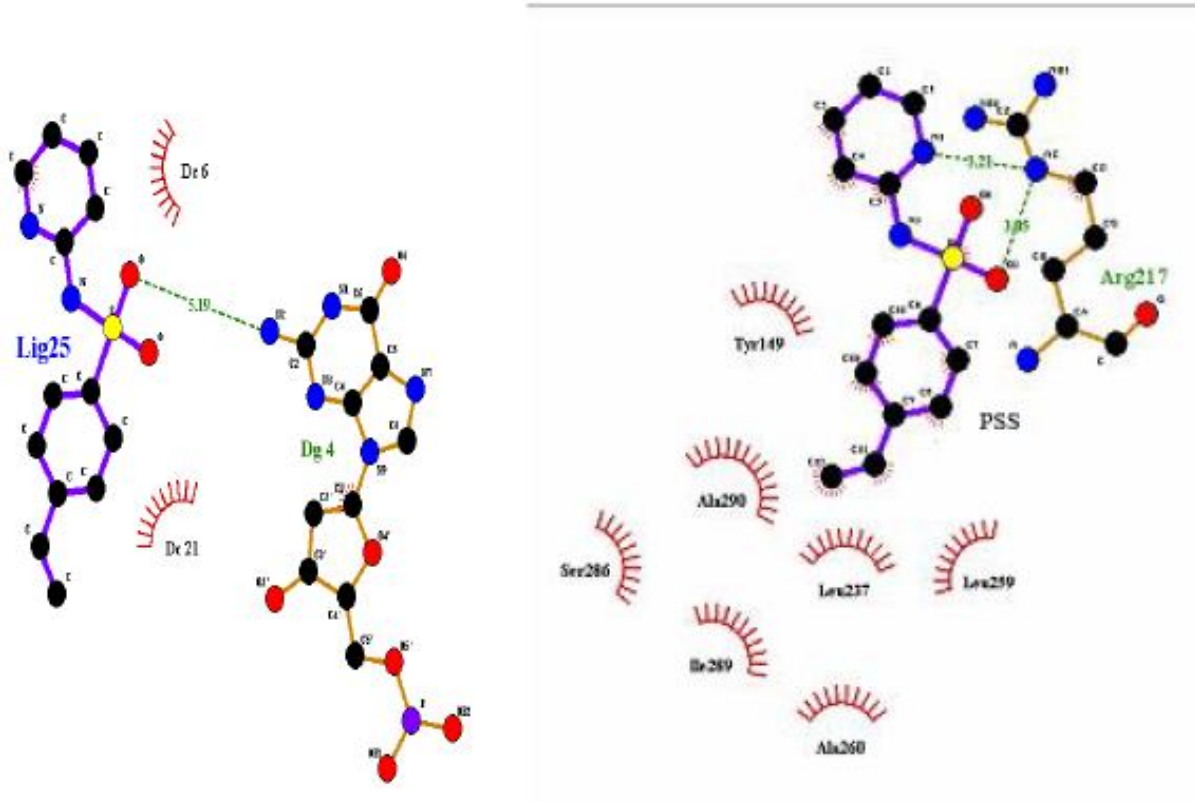

Fig. 6. (A) Perspective of molecular docking of ligand with the major groove side of DNA. The non-covalent interactions and hydrophobic forces across the binding interface of Ligand-DNA in the left and ligand-BSA in the right (H bonds are shown by green dotted lines).

Table 2. Inhibitory Zone Values (Diameter of Inhibition) from Disk Diffusion Tests

Compound	Bacteria	Inhibition zone diameter (mm)
N-(2-pyridyl)-*para*-styrene sulfonamide	E.coli	19
N-(2-pyridyl)-*para*-styrene sulfonamide	S.aureus	21

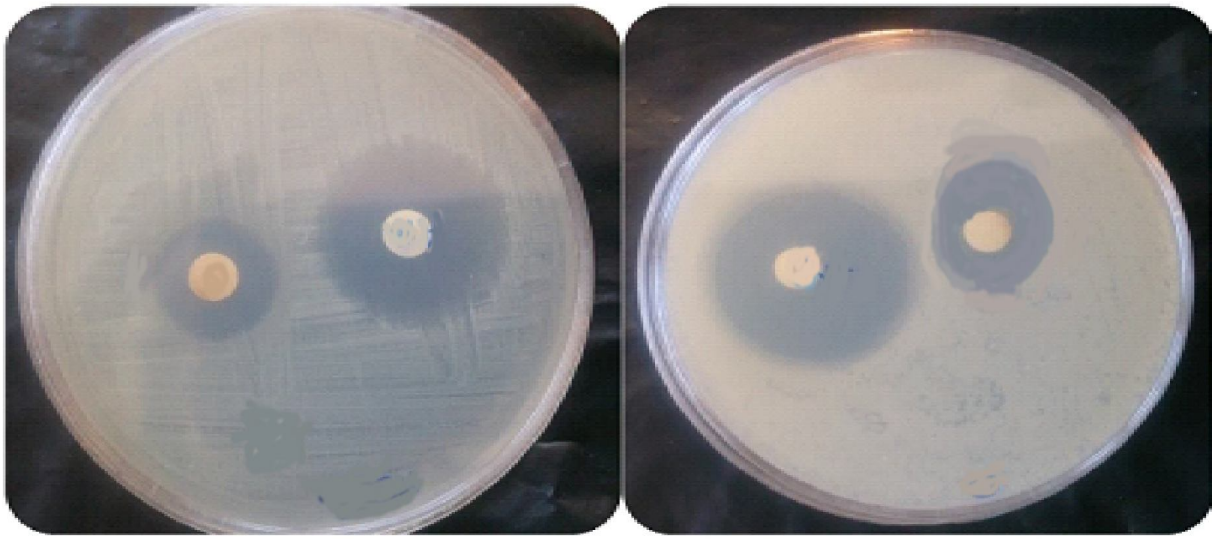

Fig. 7. The growth inhibition ring observed for ligand in S.aureus in the right and E.coli in the left.

bond (Fig. 6). This hydrogen bond is between O_{SO2} of PSS and Dg4 (5.18 Å). There are hydrophobic contacts between the carbon atoms of pyridyl ring and Dc5 and Dc21. The BSA creates two hydrogen bonds (Fig. 6). These hydrogen bonds are between $N_{pyridine}$ and Oso_2 of ligand with Arg 217(3.21 Å, 3.05 Å), respectively. There are hydrophobic contacts between the carbon atoms (C3, C4, C5, C7, C8, C10, C11, C12 and C13) of ligand with Lyr149, Leu237, Leu259, Ala260, Ser286, IIe289 and Ala290. The binding free energy (ΔG° in kcal mol^{-1}) -6.8 for DNA and -7.7 for BSA are predicted for the best conformation of the ligand. The values of ΔG° indicate a high binding affinity between DNA and BSA separately with the ligand (title compound).

The non-covalent interactions and hydrophobic forces across the binding interface of Ligand–DNA in the left and ligand-BSA in the right (H bonds are shown by green dotted lines).

The Disk Diffusion Method

A microbial suspension (1 ml) Staphylococcus aureus and Escherichia coli were spread separately over the surface of agar plate, which were then incubated for 24 h at 37 °C in an autoclave. Inhibitory zone values (diameter of inhibition) from disk diffusion tests and growth inhibition ring for PSS are reported in Table 2 and Fig. 7.

The results of this assay may indicate that both Staphylococcus aureus and Escherichia coli are sensitive to *N*-(2-pyridyl)-*para*-styrene sulfonamide, however, Staphylococcus aureus has more sensitiveness to the compounds.

CONCLUSIONS

We report the new compound of based-pyridyl sulfonamide. The molecular geometry and structural parameters of three tautomers (T_1, T_2 and T_3) were calculated using CAM-B3LYP method and Aug.-cc-pVDZ basis set. The title compound (T_1) was characterized using FT-IR, ^{1}H NMR spectroscopy. Molecular electrostatic potential and Frontier molecular orbital analyses indicated that the PSS can be designed for the new catalysts due to its properties. This research confirms the antibacterial and anticancer properties of this compound. These biological investigation results suggest that PSS can be used for the design and synthesis of the new based-drug materials.

ACKNOWLEDGMENTS

We would like to thank Lorestan University for its financial support.

REFERENCE

[1] C.T. Supuran, A. Casini, A. Mastrolorenzo, A. Scozzafava, Mini-Rev. Med. Chem. 4 (2004) 625.

[2] J. Drews, A Historical Perspective, Sci. 287 (2000) 1960.

[3] H.M. El-Shaaer, P. Foltínová, M. Lácová, J. Chovancová, H. Stankovičová, Farmaco 53 (1998) 224.

[4] Y. Genç, R. Özkanca, Y. Bekdemir, Annu. Clinic. Microbio. Antimicrob. 7 (2008) 17.

[5] N. Özbek, H. Katırcıoğlu, N. Karacan, T. Baykal, J. Bioorg. Med. Chem. 15 (2007) 5105.

[6] F. Abbate, A. Casini, T. Owa, A. Scozzafava, C.T. Supuran, J. Bioorg. Med. Chem. Lett. 14 (2004) 217.

[7] M.M. Ghorab, F.A. Ragab, M.M. Hamed, Eur. J. Med. Chem. 44 (2009) 4211.

[8] C.T. Supuran, Expert Opin. Invest. Drugs 12 (2003) 283.

[9] N.S. El-Sayed, E.R. El-Bendary, S.M. El-Ashry, M.M. El-Kerdawy, Eur. J. Med. Chem. 46 (2011) 3714.

[10] M.M. Ghorab, M. Ceruso, M.S. Alsaid, Y.M. Nissan, R.K. Arafa, C.T. Supuran, Eur. J. Med. Chem. 87 (2014) 186.

[11] A.A Mun, *et al.*, J. Med. Chem. 55 (2012) 6738.

[12] R.F. Borne, R.L. Peden, I.W. Waters, M. Weiner, R. Jordan, E.A. Coats, J. Pharm. Sci. 63 (1974) 615.

[13] A. Alsughayer *et al.*, J. Bioma.Nanobiotech. 2 (2011) 144.

[14] N.N. Al-Mohammed, *et al.*, Mol. 18 (2013) 11978.

[15] A. Al-Sughayer1, A.Z.A. Elassar, S. Mustafa, F. Al-Sagheer, J. Biomat. Nanobiotech. 2 (2011) 144.

[16] N.N. Al-Mohammed, Y. Alias, Z. Abdullah, R.M. Shakir, E.M. Taha, A.A. Hamid, Mol. 18 (2013) 11978.

[17] A. Alsughayer, A.-Z.A. Elassar, S. Mustafa, F. Al Sagheer, J. Biomat.Nanobiotech. 2 (2011) 143.

[18] Z.H. Chohan, A. Rauf, M.M. Naseer, M.A. Somra, C.T. Supuran, J. Enzyme. Inhib. Med. Chem. 21 (2006) 173.

[19] A.E. Boyd, Diabetes 37 (1988) 847.

[20] H. Kajinuma, T. Kuzuya, T. Ide, Diabetes 23 (1974) 412.

[21] F. Carta, C.T. Supuran, Expert. Opin. Ther. Pat 23 (2013) 681.

[22] A. Renzi, J. Chart, R. Gaunt, Toxic. Appl. Pharm. 1 (1959) 406.

[23] H. Kajinuma, T. Kuzuya, T. Ide, Diabetes 23 (1974) 412.

[24] S. Takayama, K. Aihara, T. Onodera, T. Akimoto, J. Toxic. Appl. Pharm. 82 (1986) 191.

[25] S. Nishikawa, J. Toxic. Sci. 8 (1983) 47.

[26] I. Becheker, H. Berredjem, N. Boutefnouchet, M. Berredjem, A. Ladjama, J. Chem. Pharm. Res. 6 (2014) 893.

[27] S.I. Alqasoumi, A.M. Al-Taweel, A.M. Alafeefy, E. Noaman, M.M. Ghorab, Eur. J. Med. Chem. 45 (2010) 738.

[28] E. Stokstad, T. Jukes, A historical Review, J. Nut. 117 (1987) 1335.

[29] N. Desideri, P. Mastromarino, C. Conti, Antivir. Chem. Chemoth. 14 (2003) 195.

[30] P. Houghton, T. Woldemariam, A. Khan, A. Burke, N. Mahmood, Antivir. Res. 25 (1994) 235.

[31] B.-T. Hong, C.-L. Chen, J.-M. Fang, K.-C. Tsai, S.-Y. Wang, W.-I. Huang, Y.-S.E. Cheng, C.-H. Wong, Bioorg. Med. Chem. 22 (2014) 6647.

[32] H. Tavakol, J. Mol. Struct: Theochem. 954 (2010) 16.
[33] H. Tavakol, M. Esfandyari, S. Taheri, A. Heydari, Spectrochimica Acta Part A: Mol. Biomol. Spect. 79 (2011) 574.
[34] A.-N.M.A. Alaghaz, H.A. Bayoumi, Y.A. Ammar, S.A. Aldhlmani, J. Mol. Struct. 1035 (2013) 383.
[35] M. Mondelli, F. Pavan, P.C. De Souza, C.Q. Leite, J. Ellena, O.R. Nascimento, G. Facchin, M.H. Torre, J. Mol. Struct. 1036 (2013) 180.
[36] B. Macías, M.V. Villa, R. Lapresa, G. Alzuet, J. Hernández-Gil, F. Sanz, J. Inorg. Biochem. 115 (2012) 64.
[37] A.Yari, E. Mehdipour, M. Karami, J. Fluoresc. 24 (2014) 1415.
[38] E. Mehdipour, H. Bahrami, Sh. Shamaei, V. Amani, B. Notash, J. Phosphorus, J. Mat. Chem. 21 (2011) 15456.
[39] E. Mehdipour, H. Bahrami, S. Shamaei, V. Amani, J. Struct. Chem. 57 (2016) 534.
[40] N. Yoda, C. Marvel, J. Poly. Sci. Part A: Gen. Papers 3 (1965) 2229.
[41] M.J. Frisch, G.W. Trucks, H.B. Schlegel, G.E. Scuseria, M.A. Robb, J.R. Cheeseman, G. Scalmani, V. Barone, B. Mennucci, GA Petersson *et al*., Gaussian, Inc., R.A. Gaussian09, 1, Wallingford CT, (2009).
[42] A.D. Becke, J. Chem. Phys. 98 (1993) 5648.
[43] S. Hirata, H. Torii, M. Tasumi, Phys. Rev. B 57 (1998) 11994.
[44] A. Lagunin, A. Stepanchikova, D. Filimonov, V. Poroikov, Bioinform. 16 (2000) 747.
[45] A. Vina, J. Comput. Chem. 31 (2010) 455.
[46] R. Huey, G.M. Morris, A.J. Olson, D.S. Goodsell, J. Comput. Chem. 28 (2007) 1145.
[47] G.M. Morris, D.S. Goodsell, R.S. Halliday, R. Huey, W.E. Hart, R.K. Belew, A.J. Olson, J. Comput. Chem. 19 (1998) 1639.
[48] A.C. Wallace, R.A. Laskowski, J.M. Thornton, Protein Eng. 8 (1995) 127.
[49] NCCLS, Methods for Dilution Antimicrobial Susceptibility Test for Bacteria that Grow Aerobically, M7- A4, in, 1997.
[50] R. G.Parr, *et al*., Electrophilicity Index, J. Am. Chem. Soc. 121 (1999) 1922.